Mehran University Research Journal of Engineering and Technology

https://doi.org/10.22581/muet1982.2401.2587

2024, 43(1) 70-81

Effect of adjusting orientation for solar energy applications in multiple climatic zones

Muhammad Uzair Yousuf [a], Muhammad Umair [b], Muhammad Rehan [c, *], Zulfiqar Ali Umrani [d]

[a] *Department of Mechanical Engineering, NED University of Engineering and Technology, Karachi Pakistan*

[b] *Department of Economics, University of Karachi, Karachi Pakistan*

[c] *Department of Electronic Engineering, Sir Syed University of Engineering and Technology, Karachi Pakistan*

[d] *Ziauddin University, Karachi Pakistan*

[*] Corresponding author: Muhammad Rehan, Email: murehan@ssuet.edu.pk

Received: 14 October 2022, Accepted: 20 December 2023, Published: 01 January 2024

KEYWORDS

Solar

Optimum

Tilt

Azimuth

Contour

Perez

ABSTRACT

South-facing collectors are the optimum choice for solar applications in the northern hemisphere. However, obstacles may limit the feasibility of this orientation. Therefore, altering the orientation of the collector impacts solar insolation. In this study, the Perez model is utilized to evaluate incoming solar radiation on tilted surfaces for solar collectors in four climatic zones across Pakistan. The results are presented in contour plots to analyze the optimal tilt and orientation for solar applications. The findings of the study indicate substantial energy gains when collectors are placed at optimum angles. More specifically, Quetta leads with a 14.54% increase, followed by Karachi and Multan at 9.81% and 9.3%, respectively, compared to horizontally placed collectors. Analysis of vertical surfaces reveals a notable decrease in monthly solar radiation, especially in Peshawar (37.22%). Monthly adjustments in tilt angles outperform fixed positions, enhancing solar energy intensity. When comparing yearly adjustments with monthly adjustments, Quetta shows the maximum increase of 5.92%, followed by Karachi (4.86%), Multan (4.01%), and Peshawar (3.65%). It is also observed that ±15° azimuth angle change from the south ensures receiving up to 98% of insolation, regardless of the climatic region. Lastly, the validation against the NASA SSE database further highlights the reliability of our simulation model. Overall, the outcomes of the study will contribute to informed solar energy planning in the studied regions.

1. Introduction

The environmental impact of using fossil fuels raises serious concerns. Conventional power plants reliant on fossil fuels contribute significantly to the escalating levels of greenhouse gas emissions and air pollution [1]. These environmental challenges highlight the necessity to shift towards renewable energy sources. Among renewable sources, solar energy is distinctive not just for its cleanliness and sustainability but also for its transformative potential in reshaping our energy landscape. Unlike finite fossil fuels, solar power harnesses the virtually boundless energy of the sun,

offering an eco-friendly and perpetually available resource to meet our increasing energy demands.

Solar insolation, representing the amount of sunlight received, is fundamental to the efficiency of solar technologies [2]. A thorough understanding and maximization of solar insolation are essential for advancing the practicality and effectiveness of solar applications. While employing a tracking system stands out as the optimal method for continuously optimizing the collector's position, this approach is often hindered by its cost and may not always be an economically viable solution. Therefore, a frequently adopted strategy to maximize solar insolation involves affixing the collector at an optimal tilt angle and orientation [3].

Numerous studies have been conducted globally to determine the optimal positioning of solar collectors. These methodologies relying on either mathematical models [4] or measured solar data [5]. Hussein et al. [6] explored theoretical PV module performance in Egypt, proposing tilt angles within the range of 20° to 30° facing south. Skeiker [7] utilized a mathematical model to calculate an optimum tilt angle, recommending adjustments 12 times a year for maximum solar radiation. These monthly adaptations were estimated to yield approximately 30% more solar radiation than collectors placed horizontally.

Elminir et al. [8] assessed three anisotropic models to identify the best-suited sky model and optimal tilt angles, with their results highlighting the superiority of the Perez model. Benghanem [9] conducted a case study in Saudi Arabia, concluding that yearly adjustments incurred an 8% loss compared to monthly adjustments. Jafarkazemi and Saadabadi [10] investigated optimum angles for solar applications in Abu Dhabi, determining that the annual optimum tilt angle coincided with the latitude angle oriented toward the south. They found that adjusting the tilt angle twice a year resulted in higher radiation reception.

Further analyses indicated energy increases with monthly, seasonal, and yearly optimum tilt angles. The study conducted by Despotovic et al. [11] showed a 15.42%, 13.55%, and 5.98% increase in collected energy by placing panels at monthly, seasonal, and yearly optimum tilt angles, respectively. Kaddoura et al. [5] examined the optimum tilt angle for seven cities in Saudi Arabia using NASA data, validating negative tilt angles for summer and suggesting their viability as optimal tilt angles.

Roux [12] utilized measured data to assess optimum angles for nine stations in South Africa, revealing that optimally-fixed collectors captured 10% more annual solar insolation than horizontally-fixed collectors. Various correlations are addressed in the literature, such as $\phi - 3.5°$ [13], $\phi \pm 15°$ [8], $\phi - \delta$ [4], $0.917\phi + 0.321$ [14]. The positive sign is employed for the winter season, whereas the negative sign is used for the summer season.

In accordance with the aforementioned findings, it is established that optimal orientation for solar collectors in the northern hemisphere is facing south. However, practical constraints often render south-oriented placements unfeasible. Subsequently, alterations in collector orientation impact the determination of optimum tilt angles [15]. The aim of this study is to fill this gap by assessing the optimal tilt and azimuth angles for solar collectors in four major cities in Pakistan, each representing distinct climates. The objective is to understand how alterations in collector orientation, influenced by practical constraints, affect the determination of optimum tilt angles.

In this study, we employed ground measurement data obtained through highly calibrated pyranometers for four major cities in Pakistan, each representing distinct climates. The utilization of ground measured data underscores the significance of our work. Notably, research indicates an increase in dense foggy days and a notable shift in aerosol concentration in specific regions of Pakistan post-2008 [16, 17].

The Perez Model served as the primary tool for estimating solar irradiation on inclined surfaces, considering multiple orientations at various tilt angles. The methodology was formulated using MATLAB software. Afterwards, contour plots were generated to facilitate the installation of a series of solar applications. As Pakistan does not contain extensive urban mesh, thus this analysis assumes no change in the diffuse sky view factor due to adjacent buildings and obstacles.

2. Materials and Methods

In this section, a comprehensive research framework and design of our methodology is explained. The investigation is initiated with solar radiation measurements, where calibrated pyranometers are utilized to ensure accuracy and reliability in the acquired data. Afterward, the four major cities across Pakistan are selected representing the diversified climatic conditions. In this study, Perez Model is considered to estimate solar irradiation on inclined surfaces. The model is thoroughly explained and is programmed in MATLAB, utilizing Intel i5, 1.70 GHz quad-core processor with 16 GB RAM. The programming provides a mathematical

framework essential for estimating monthly solar irradiation on inclined surfaces. Finally, the estimated solar irradiation was considered to determine the optimum tilt and azimuth angles for multiple conditions.

2.1 Solar Radiations Measurements

In recent years, the World Bank initiated renewable energy resource mapping as a part of Energy Sector Management Assistance Program (ESMAP) in Pakistan. The program specifically concentrated on assessing three key renewable resources: solar, biomass, and wind.

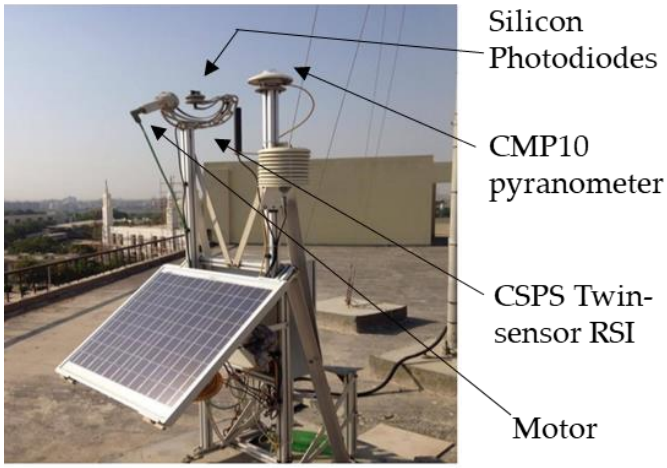

Fig. 1. Tier 2 weather station installed at NEDUET, Karachi [18]

Table 1

Uncertainties of the measurement equipment

Parameter	Instrument	Model	Uncertainty
GHI	Pyranometer	CMP10	±3%
GHI and DHI	Twin sensor Rotating Shadowband Irradiometer	CSPS	(daily)
Wind Direction	Wind vane	NRG #200P	Dead Band (356° to 4°) ±4.3° (> 4° to < 356°)
Wind Speed	Anemometer	NRG #40C	±1.48%
Relative Humidity	temperature and relative humidity probe	CS215	±2% over 10–90% (at 25°C) ±4% over 0–100% (at 25°C)
Air temperature		CS215	±0.3°C at 25°C ±0.4°C over 5–40°C ±0.9°C over -40–70°C

As part of this initiative, nine weather stations were installed throughout the country. In our study, Tier 2 weather station is considered as depicted in Fig. 1. The station is equipped with advanced instrumentation including a Campbell Scientific CR1000 data logger, Kipp and Zonen CMP10 pyranometer, CSPS Twin-sensor RSI, CS100 barometric pressure sensor, and CS215 temperature and relative humidity probe. Additionally, the station features a wind tower positioned at a height of 10 meters.

For daily irradiation measurements, the station maintains a measurement uncertainty of approximately < 3%. Data collection is facilitated through the use of GPRS technology. The uncertainties of the measurement equipment [19] are shown in Table 1.

2.2 Selected Cities

Given its geographical coordinates, Pakistan spans approximately between latitudes 24°N to 37°N and longitudes 62°E to 75°E. For this study, we selected four stations, taking into consideration the diverse climatic zones present in the country [20]. Fig. 2 provides a visual representation of the details pertaining to these selected stations.

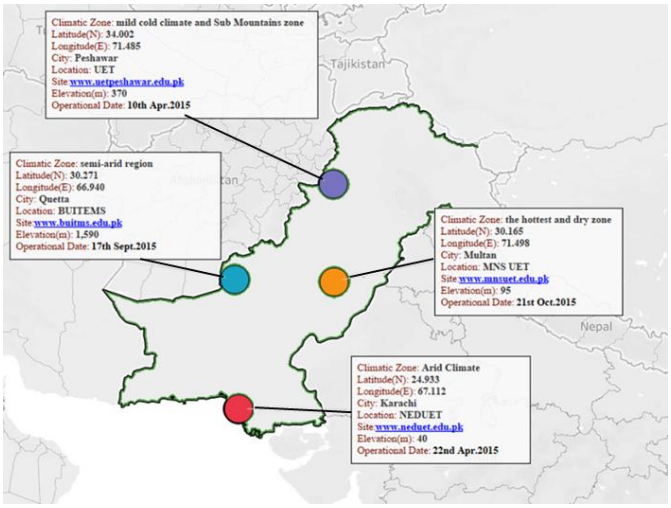

Fig. 2. Weather Stations installed in selected cities

2.3 Mathematical model

The geometric relationship between the location of the sun and a plane with respect to the earth at any given time is defined by a number of angles [21]. The hour angle (ω) is expressed as

$$\omega = (Solar\ Time - 12)\ \text{x}\ 15 \quad (1)$$

It is the angular displacement of the sun (east or west of the local meridian) caused by the rotation of the Earth on its axis at a rate of 15° per hour [22].

The declination angle (δ), as shown in eq (2), is calculated using an approximation of Cooper's equation.

$$\delta = 23.45\, sin\left(360 \times \frac{284+n}{365}\right) \quad (2)$$

where 1 ≤ n ≤ 365. It represents the angular position of the sun with respect to the plane of the equator at solar noon [22]. The solar altitude (α_s) and azimuth (γ_s) angles are determined as in Eq. (3) and (4).

$$\alpha_s = sin^{-1}(sin\,\delta\, sin\,\phi + cos\,\delta\, cos\,\phi\, cos\,\omega) \quad (3)$$

$$\gamma_s = sign\,(\omega)\left|cos^{-1}\left(\frac{cos\,\theta_Z\, sin\,\phi - sin\,\delta}{sin\,\theta_Z\, cos\,\phi}\right)\right| \quad (4)$$

where $\theta_z = 90 - \alpha_s$. These solar angle calculations help in locating the sun for every hour of the year. The angle of incidence of beam radiation (θ) on a surface, shown in (5), can be used to relate these angles.

$$cos\,\theta = sin\,\delta\, sin\phi\, cos\,\beta - sin\,\delta\, cos\,\phi\, sin\,\beta\, cos\,\gamma + cos\,\delta\, cos\,\phi\, cos\,\beta\, cos\,\omega + cos\,\delta\, sin\,\phi\, sin\,\beta\, cos\,\gamma\, cos\,\omega + cos\,\delta\, sin\,\beta\, sin\,\gamma\, sin\,\omega \quad (5)$$

The solar radiation incident on a horizontal plane, at any point in time, outside the atmosphere (extraterrestrial) is evaluated from

$$I_o = I_{SC}\left(1 + 0.033\cos\frac{360\,n}{365}\right)\cos\theta_z \quad (6)$$

where I_{SC}=1367 W/m^2 is the solar constant. The hourly horizontal extraterrestrial radiation is calculated from:

$$I_o = \frac{12}{\pi} I_{SC}\left(1 + 0.033\cos\frac{360\,n}{365}\right) \text{x}\,[\,cos\,\delta\, cos\,\phi\,(\sin\omega_2 - \sin\omega_1) + \frac{2\pi(\omega_2-\omega_1)}{360} sin\,\phi\, sin\,\delta\,] \quad (7)$$

2.4 Perez model

Various models have been developed to calculate solar irradiation on surfaces with different tilt angles and orientations based on data for horizontal surfaces. Among the three components – direct irradiation, ground-reflected irradiation, and sky diffuse irradiation – the calculation of direct irradiation is geometric and consistent across models i.e. $I_b R_b$. For ground-reflected irradiation, the isotropic assumption is commonly used in many studies, and it is estimated using $I\rho_g[1 - \cos\,\beta)/2]$. The key difference between these models lies in how they consider the sky diffuse irradiation component.

Among different models, Perez model is frequently employed and cited as one of the best performing models [23, 24]. Perez model [25] takes all the three diffuse components: isotropic, horizon brightening, and circumsolar. It is also used as a proxy radiation method in PVFORM to predict load matching capability of twenty United States utilities [26].

The generalized Perez model to evaluate the total solar irradiation is defined as:

$$I_T = I_b R_b + I_d(1 - F_1)\left(\frac{1+cos\,\beta}{2}\right) + I_d F_1 \frac{a}{b} + I_d F_2\, sin\,\beta + I\rho_g\left(\frac{1-cos\,\beta}{2}\right) \quad (8)$$

The term R_b is a geometric factor and is defined as:

$$R_b = \frac{I_{bT}}{I_b} = \frac{I_{bn}\, cos\,\theta}{I_{bn}\, cos\,\theta_z} = \frac{cos\,\theta}{cos\,\theta_z} \quad (9)$$

The parameters a and b, calculated as $\max(0, \cos\theta)$ and $\max(\cos 85\,, \cos\theta_z)$, are the angles of incidence of the cone for circumsolar radiation on inclined and horizontal surfaces. Please note that during most of the hours, the expression a/b simplifies to R_b. The circumsolar and horizon brightening coefficients, denoted by F_1 and F_2, are dependent on three sky condition parameters: zenith angle (θ_z), clearness (ε), and brightness (Δ). Clearness (ε) and brightness (Δ) are given as:

$$\varepsilon = \frac{\frac{DHI+DNI}{DHI} + 5.535\times10^{-6}\theta_z{}^3}{1 + 5.535\times10^{-6}\,\theta_z{}^3} \quad (10)$$

$$\Delta = m\,\frac{DHI}{I_{on}} \quad (11)$$

Referring to Eq. (11), m is the Air Mass (A.M.), and I_{on} is the extraterrestrial normal-incidence radiation and is calculated using Eq. (12) and (13) [27, 28] respectively

$$m = \frac{1}{cos\,\theta_Z} \quad (12)$$

$$I_{on} = I_{SC}(1.000110 + 0.034221 cosB + 0.001280 sinB + 0.000719 cos2B + 0.000077 sin2B) \quad (13)$$

Where, $B = (n-1)\frac{360}{365}$

The brightness coefficients F_1 and F_2 in the Perez Model were generated from six factors coefficients F_{ij}. Based on eight brightness bins for a range of clearness (as given in Table 2), the F_{ij} were selected. The factors F_1 and F_2 are evaluated as:

$$F_1 = max\,[0, (f_{11} + f_{12}\Delta + \frac{\pi\theta_z}{180} f_{13})] \quad (14)$$

$$F_2 = (f_{21} + f_{22}\Delta + \frac{\pi\theta_z}{180} f_{23}) \quad (15)$$

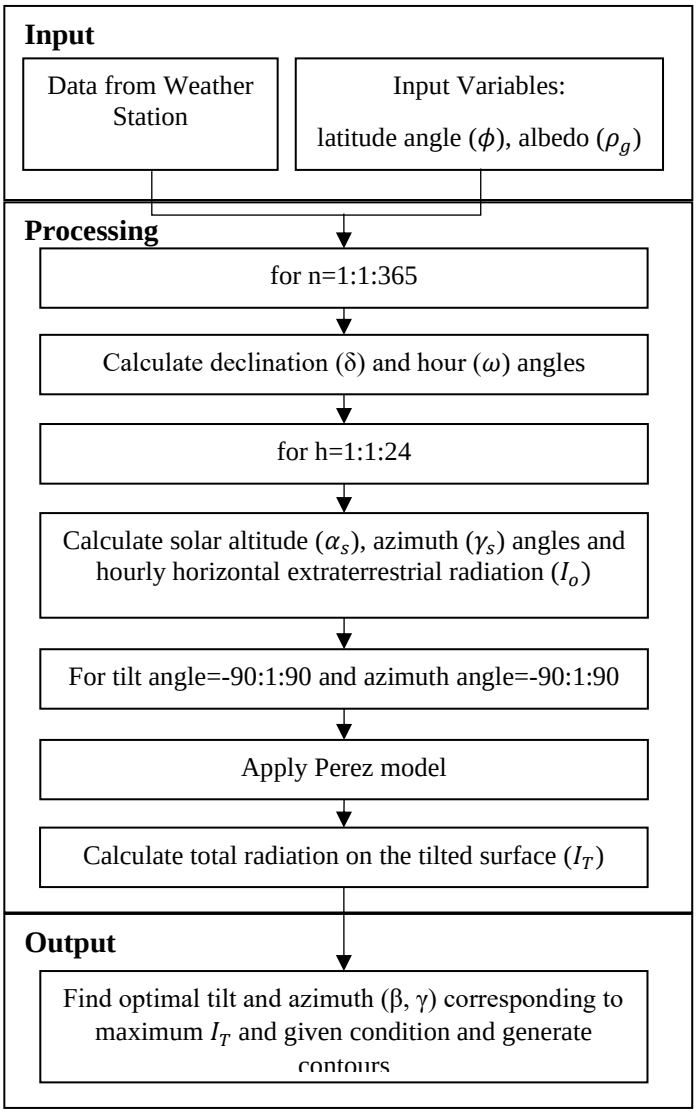

Fig. 3. Flowchart depicting the overall methodology

Table 2

Coefficients for Perez Model Fij parameters

Range of ε	**f_{11}**	**f_{12}**	**f_{13}**	**f_{21}**	**f_{22}**	**f_{23}**
1.000–1.065	−0.008	0.588	−0.062	−0.060	0.072	−0.022
1.065–1.230	0.130	0.683	−0.151	−0.019	0.066	−0.029
1.230–1.500	0.330	0.487	−0.221	0.055	−0.064	−0.026
1.500–1.950	0.568	0.187	−0.295	0.109	−0.152	0.014
1.950–2.800	0.873	−0.392	−0.362	0.226	−0.462	0.001
2.800–4.500	1.132	−1.237	−0.412	0.288	−0.823	0.056
4.500–6.200	1.060	−1.600	−0.359	0.264	−1.127	0.131
6.200–∞	0.678	−0.327	−0.250	0.156	−1.377	0.251

The usual approach for the calculation of the diffuse component is to correlate I_d/I, with the hourly clearness index ($k_t = \frac{I}{I_o}$). The commonly used Erb's correlation [29] is defined as:

$$\frac{I_d}{I} = \begin{cases} 1 - 0.09\,k_t & for\ k_t \le 0.22 \\ 0.9511 - 0.1604\,k_t + 4.388{k_t}^2 - 16.638{k_t}^3 + 12.336{k_t}^4 & for\ 0.22 \le k_t \le 0.80 \\ 0.165 & for\ k_t > 0.80 \end{cases} \quad (16)$$

Also, the beam radiation is calculated as

$$I_b = I - I_d \quad (17)$$

The set of Eq. from 9 to 17 will help in the calculation of total radiation on the tilted surface using Eq. 8.

2.4 Optimum tilt and azimuth angles

The mathematical model discussed was utilized to calculate optimum angles for the collector, varying between -90° ≤ (β, γ) ≤ 90° in intervals of 1°. All calculations were carried out monthly. A collector with an azimuth angle of 0° is south facing. Therefore, a negative azimuth angle indicates the collector's rotation from south to east, while the opposite case applies from south to west.

For all selected locations, the most favorable combinations of tilt and azimuth angles were determined. The proposed methodology was implemented in MATLAB to generate contour plots. Contour plots serve as a convenient means to illustrate the impact of tilt angle and orientation on annual solar radiation [12, 30]. Fig. 3 shows the overall methodology applied in this study.

3. Simulation and Results

The methodology employed involved a step-by-step procedure, starting with the acquisition of data from a weather station. The processing phase involved a calculation sequence. For each day of the year (n=1 to 365), declination (δ) and hour (ω) angles were calculated, laying the foundation for determining solar altitude (α_s), azimuth (γ_s) angles, and hourly horizontal extraterrestrial radiation (I_o) for each hour of the day (h=1 to 24).

The critical step in our methodology was the application of the Perez model, executed for a range of tilt and azimuth angles (-90° to 90°). This model allowed us to calculate the total radiation on the tilted surface (I_T) for each combination of tilt and azimuth angles. The output of this process was a comprehensive dataset that facilitated the identification of optimal tilt and azimuth angles (β, γ) corresponding to maximum total radiation (I_T).

The simulations were conducted for two scenarios.

In the first scenario, simulations were conducted with horizontally placed collectors, maintaining a fixed azimuth angle while varying the tilt angle. This scenario explains the optimal tilt angle for maximizing radiation under fixed azimuth conditions. The second scenario involved collectors with tilt angles equivalent to latitude angles, keeping the tilt angle fixed but varying the azimuth angle. This scenario explores the influence of changing azimuth angles on solar energy capture. For applications where a fixed azimuth orientation is desirable, the first scenario informs the optimal tilt angle adjustments for maximizing energy capture. On the other hand, the second scenario caters to situations where the tilt angle remains constant, offering guidance on the azimuth orientation that aligns with the latitude for enhanced solar energy harvesting. The outcomes of these simulations are shown in Fig. 4 (a to h).

The analysis of Fig. 4 (a to h) shows a significant increase in maximum annual energy when the collector faces south with a tilt angle equal to latitude, as opposed to a horizontal placement. In general, the visual analysis of regional contour plots reveals that adjusting the collector position has the most pronounced impact on the semi-arid region, followed by the arid climate and the dry zone, while the mild cold climatic zone experiences the least impact. This finding underscores the varying sensitivity of solar energy capture to collector positioning across different climatic zones in the studied regions of Pakistan. The semi-arid region, characterized by distinct weather patterns, exhibits a more substantial response to changes in collector orientation, emphasizing the need for tailored approaches in optimizing solar energy efficiency based on regional climate conditions.

Moreover, a significant inference drawn from the contour plots is that varying the azimuth angle by ±15° from the south yields solar insolation levels within 98% of those achieved with a south-facing orientation. This result suggests that, within this azimuthal range, there is a relatively small loss in insolation, highlighting a practical flexibility in collector positioning. Such insight can inform more practical and feasible installations, considering that deviations within this range still offer an efficient utilization of solar resources. This finding may contribute to the development of cost-effective solar energy systems, especially in regions where the strict adherence to a south-facing orientation is not always feasible due to practical constraints.

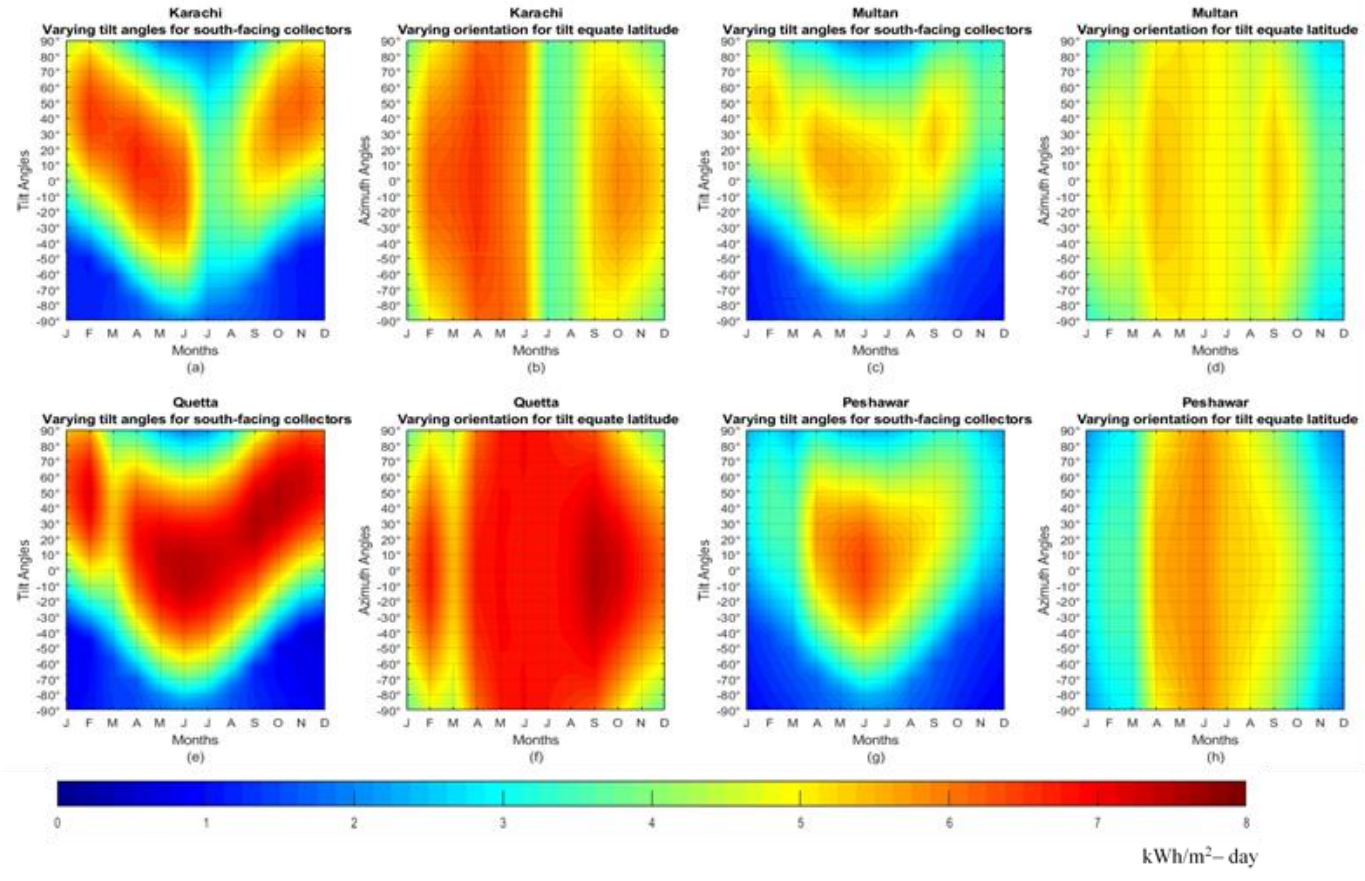

Fig. 4. Contour plot of monthly average daily radiation for Karachi a) at a varying tilt for south-facing collector b) at varying azimuth for tilt equate latitude angle, Multan c) at varying tilt for south-facing collector d) at varying azimuth for tilt equate latitude angle, Quetta e) at varying tilt for south-facing collector f) at varying azimuth for tilt equate latitude angle, Peshawar g) at varying tilt for south-facing collector h) at varying azimuth for tilt equate latitude angle.

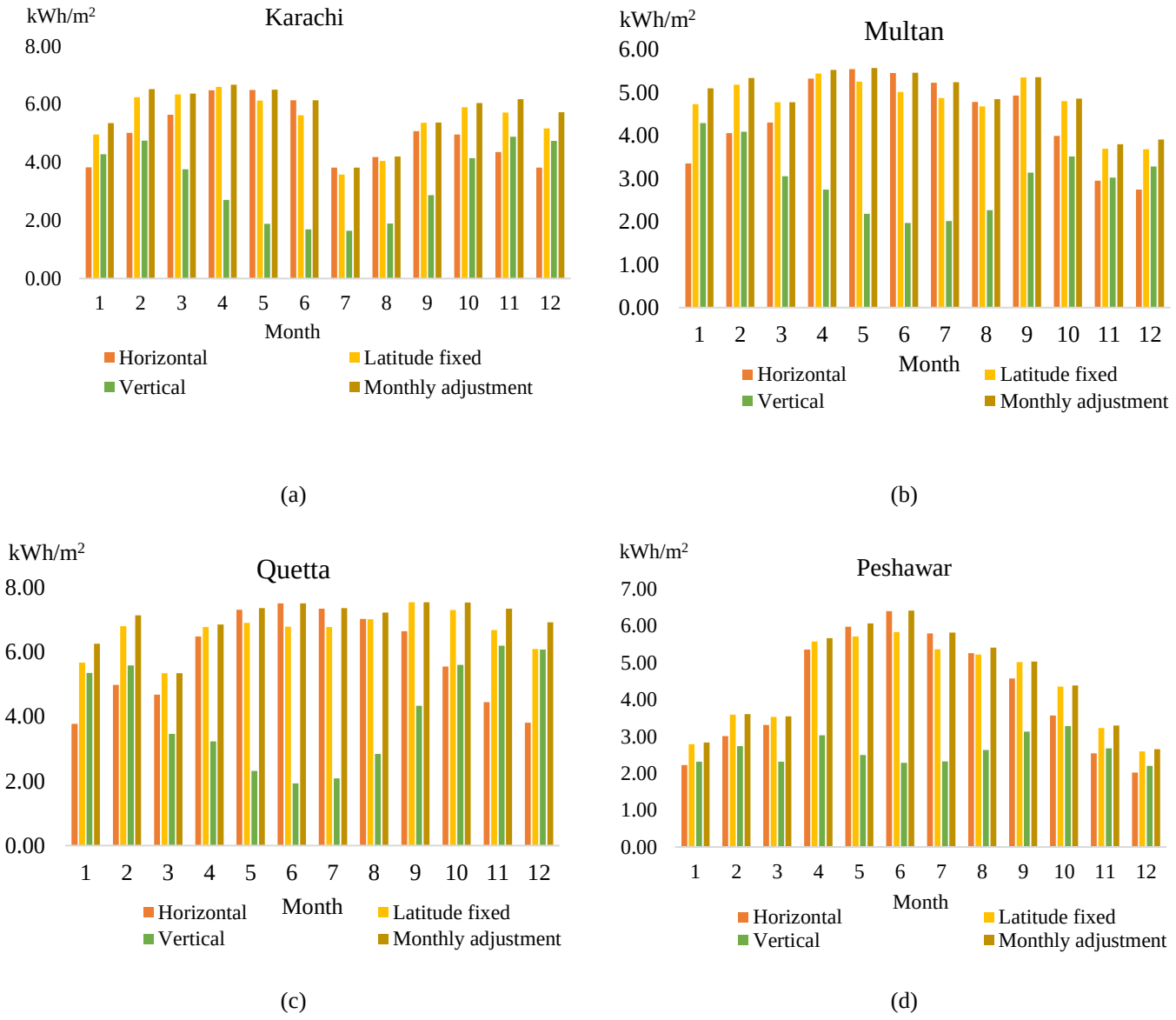

Fig. 5. Global solar insolation for horizontal, latitude-equated tilt, vertical, and monthly adjustment facing south for (a) Karachi (b) Multan (c) Quetta (d) Peshawar.

The detailed contour plots for each city are provided in annexure (Fig. 6.1 – 6.4). These comprehensive visual representation highlights the considerable advantages of dynamic adjustments in tilt angles throughout the year, emphasizing the potential for significantly increased solar energy capture in diverse climatic zones.

To provide a detailed comparison of maximum solar insolation received in different scenarios, Fig. 5 illustrates the outcomes for horizontal, latitude-equated tilt, vertical, and monthly adjustment positions extracted from contour plots.

As seen in Fig. 5, Quetta exhibits the most substantial difference, with a 14.54% increase, followed by Karachi and Multan, showcasing variations of 9.81% and 9.3%, respectively. Peshawar, on the other hand, demonstrates the minimum difference, with a 5.56% increase in annual energy.

It is pertinent to note that Building Integrated Photovoltaic (BIPV) panels are of particular interest and widely used globally. The plotted contours help in exploring solar radiation for south-facing collectors on vertical surfaces. The analysis reveals that the monthly solar radiation received by vertical surfaces is considerably lower than that received by horizontal surfaces. Peshawar exhibits the maximum difference, with a 37.22% decrease, followed by Karachi and Multan, with variations of 34.37% and 32.49%, respectively. In contrast, Quetta shows the minimum difference, with a 29.56% decrease in annual energy.

Furthermore, it is observed that the amount of solar radiation received during summer months surpasses that received during winter months due to the higher altitudes of the sun. This seasonal variation is consistent with expectations based on solar geometry.

Further to analyze the effect of adjusting tilt angles 12 times a year to optimize solar energy intensity, the simulations were conducted varying both tilt and azimuth angles monthly. The resulting contour plots, available in the supplementary material (Fig. 6.1 – 6.4), reveal that altering the tilt angle of south-facing collectors 12 times leads to a significant increase in solar energy intensity compared to horizontal placement. Fig. 5 concludes that Quetta receives 21.32% more energy than horizontally placed collectors, followed by Karachi, Multan, and Peshawar, which collect 15.15%, 13.51%, and 9.42% more energy, respectively. When compared with the latitude-equated tilt angles and those varied 12 times a year, Quetta shows the maximum increase of 5.92%, followed by Karachi with 4.86%, Multan with 4.01%, and Peshawar with 3.65%.

The simulated angles are also compared with the NASA SSE database [31]. The database provides mean daily values for meteorological parameters and solar irradiation in a time series format. These datasets are derived from rigorous satellite observations and robust model-based simulations. Thorough validation has attested to the high accuracy of these products, ensuring their dependability in delivering solar and meteorological resource data. This is particularly advantageous in regions where surface measurements are scarce or unavailable. Due to the higher accuracy, many softwares such as RETScreen, BlueSol 4, and Homer Grid utilize these solar radiation data for clean energy project analysis and feasibility studies.

Table 3 provides a comprehensive overview of the comparison results, presenting the corresponding monthly average daily values. The comparison between optimum tilt angles from NASA SSE database and the simulated results for Karachi, Multan, Quetta, and Peshawar provides valuable insights into the accuracy of the simulation model. In Karachi, βopt from NASA ranges from 0° to 52°, closely mirrored by the simulation with values ranging from 0° to 53°. For Multan, βopt from NASA varies from 0° to 56°, and the simulation closely follows with values ranging from 0° to 52°. In Quetta, βopt from NASA ranges from 0° to 57°, and the simulation closely mirrors this trend with values ranging from 0° to 60°. In Peshawar, βopt from NASA varies from 0° to 61°, while the simulation aligns closely with values ranging from 0° to 49°. While there are some minor variations in angles, the simulation results generally follow the trend of NASA showcasing its ability to capture variations across different months. In general, the simulation closely aligns with NASA values for optimum tilt, demonstrating a good agreement.

Table 3

Monthly optimum tilt angle from the simulation and NASA SSE database for validation

City	Database	Values	Month											
			Jan	Feb	Mar	Apr	May	Jun	Jul	Aug	Sep	Oct	Nov	Dec
Karachi	NASA	β_{opt}(°)	50	42	27	12	0	0	0	6	20	37	47	52
	Simulation	β_{opt}(°)	49	43	30	15	3	0	0	6	22	38	49	53
		I_T (kWh/m^2)	5.35	6.52	6.37	6.67	6.5	6.13	3.82	4.2	5.37	6.04	6.17	5.73
Multan	NASA	β_{opt}(°)	54	46	31	16	2	0	0	9	25	42	52	56
	Simulation	β_{opt}(°)	54	45	30	18	7	2	4	11	27	40	46	52
		I_T (kWh/m^2)	5.1	5.34	4.78	5.53	5.58	5.46	5.24	4.85	5.36	4.86	3.8	3.91
Quetta	NASA	β_{opt}(°)	55	47	32	17	2	0	0	10	27	43	53	57
	Simulation	β_{opt}(°)	57	49	33	21	8	0	5	15	30	45	56	60
		I_T (kWh/m^2)	6.26	7.14	5.35	6.85	7.37	7.51	7.37	7.23	7.54	7.54	7.34	6.92
Peshawar	NASA	β_{opt}(°)	58	48	35	19	6	0	3	13	30	47	57	61
	Simulation	β_{opt}(°)	47	41	27	22	11	5	6	16	29	41	47	49
		I_T (kWh/m^2)	2.84	3.61	3.55	5.67	6.07	6.42	5.82	5.41	5.03	4.38	3.29	2.66

In summary, our investigation of optimal tilt and azimuth angles for solar collectors in major Pakistani cities reveals significant energy gains, with Quetta leading at 14.54% increase, followed by Karachi and Multan at 9.81% and 9.3%. Analysis of Building Integrated Photovoltaic (BIPV) panels on vertical surfaces demonstrates decreased monthly solar radiation, with Peshawar exhibiting the highest difference (37.22%). Seasonal variation follows solar geometry expectations, favoring increased radiation during summer months. Monthly adjustments in tilt angles outperform fixed positions, enhancing solar energy intensity. Comparing latitude-equated tilt angles adjusted 12 times a year, Quetta shows the maximum increase of 5.92%, followed by Karachi with 4.86%, Multan with 4.01%, and Peshawar with 3.65%. Validation against NASA SSE database highlights the reliability of our simulation model, providing a robust basis for strategic solar energy planning in the studied regions. Overall, these findings contribute valuable insights for informed solar energy planning in the studied regions.

4. Conclusion

In conclusion, this study provides vital insights into optimizing solar collector orientation in four major cities of Pakistan—Karachi, Multan, Quetta, and Peshawar. The key findings emphasize the importance of location-specific adjustments, with optimal tilt angles varying for each city. Notably, the months of June and December stand out as periods with the lowest and highest optimal tilt angles, indicating their crucial influence on energy capture efficiency.

The effectiveness of collectors with latitude-equated tilt angles facing south throughout the year is highlighted. This approach results in a notable increase in annual solar irradiation, with Quetta, Karachi, Multan, and Peshawar showcasing varying degrees of energy gain, with increases of 21.32%, 15.15%, 13.51%, and 9.42%, respectively. The study highlights the significance of azimuth angle variations, as revealed by contour plots illustrating the impact of fixed tilt and azimuth angles on monthly solar insolation. More specifically, varying the azimuth angle by ±15° from the south will provide almost 98% of the insolation as the south orientation. This information is invaluable for designing cost-effective solar applications.

Moreover, the study draws attention to the considerable difference in monthly solar radiation between vertical and horizontal surfaces. This shows up the importance of strategic collector orientation for maximizing energy capture and efficiency.

Based on the findings, specific recommendations emerge from this research. Firstly, solar collectors should be tailored to the optimal tilt and azimuth angles identified for each city. However, if adjustment at optimum tilt angle is not possible then incorporate azimuth angle variations in solar installations to enhance solar insolation and overall energy capture.

The outcome of this study provides implications for integrating solar energy solutions into city planning. Also, these results contribute to accelerate the transition to renewable energy sources in Pakistan, mitigating the impact of electricity shortages and fostering a more robust and sustainable energy landscape.

A limitation of this study arises from the assumption that the diffuse sky view factor remains unchanged due to the limited urban development in Pakistan. For future work, exploring the applicability of these results to urban environments with intense urban mesh and delving into the impacts of seasonal adjustments and shading effects could provide valuable insights.

5. Availability of Data and Materials

The NASA and ESMAP repository contains the datasets analyzed during the current investigation.

Nomenclature

AEDB	Alternative Energy Development Board
DHI	Diffuse Horizontal Irradiation
ESMAP	Energy Sector Management Assistance Program
I_b	Beam radiation on the horizontal (kWh/m^2)
I	Global radiation on the horizontal (kWh/m^2)
NASA	National Aeronautics and Space Administration
PV	Photovoltaic
RSI	Rotating Shadowband lrradiometer
CSP	Concentrated Solar Power
DNI	Direct Normal Irradiation
GHI	Global Horizontal Irradiation
I_d	Diffuse radiation on the horizontal (kWh/m^2)
I_T	Insolation on a tilted surface (kWh/m^2)
NEPRA	National Electric Power Regulatory Awuthority
R_b	Geometric factor

SSE	Surface Meteorology and Solar Energy
Greek	
α_s	Sun altitude angle (in degrees)
γ_s	Sun azimuth angle (in degrees)
θ_z	Zenith angle (in degrees)
ϕ	Latitude (in degrees)
Δ	brightness
ϕ	Slope or tilt angle (in degrees)
δ	Declination angle (in degrees)
ρ_g	Surface albedo
ω	Hour angle (in degrees)
ε	clearness

6. References

[1] M. Umair and M. U. Yousuf, "Evaluating the symmetric and asymmetric effects of fossil fuel energy consumption and international capital flows on environmental sustainability: a case of South Asia," Environmental Science and Pollution Research, vol. 30, no. 12, pp. 33992-34008, 2023.

[2] A. Ullah, H. Imran, Z. Maqsood, and N. Z. Butt, "Investigation of optimal tilt angles and effects of soiling on PV energy production in Pakistan," Renewable Energy, vol. 139, pp. 830-843, 2019.

[3] H. Zang, M. Guo, Z. Wei, and G. Sun, "Determination of the optimal tilt angle of solar collectors for different climates of china," Sustainability, vol. 8, no. 7, p. 654, 2016.

[4] C. Stanciu and D. Stanciu, "Optimum tilt angle for flat plate collectors all over the World–A declination dependence formula and comparisons of three solar radiation models," Energy Conversion and Management, vol. 81, pp. 133-143, 2014.

[5] T. O. Kaddoura, M. A. Ramli, and Y. A. Al-Turki, "On the estimation of the optimum tilt angle of PV panel in Saudi Arabia," Renewable and Sustainable Energy Reviews, vol. 65, pp. 626-634, 2016.

[6] H. Hussein, G. Ahmad, and H. El-Ghetany, "Performance evaluation of photovoltaic modules at different tilt angles and orientations," Energy conversion and management, vol. 45, no. 15, pp. 2441-2452, 2004.

[7] K. Skeiker, "Optimum tilt angle and orientation for solar collectors in Syria," Energy Conversion and Management, vol. 50, no. 9, pp. 2439-2448, 2009.

[8] H. K. Elminir, A. E. Ghitas, F. El-Hussainy, R. Hamid, M. Beheary, and K. M. Abdel-Moneim, "Optimum solar flat-plate collector slope: case study for Helwan, Egypt," Energy Conversion and Management, vol. 47, no. 5, pp. 624-637, 2006.

[9] M. Benghanem, "Optimization of tilt angle for solar panel: Case study for Madinah, Saudi Arabia," Applied Energy, vol. 88, no. 4, pp. 1427-1433, 2011.

[10] F. Jafarkazemi and S. A. Saadabadi, "Optimum tilt angle and orientation of solar surfaces in Abu Dhabi, UAE," Renewable energy, vol. 56, pp. 44-49, 2013.

[11] M. Despotovic and V. Nedic, "Comparison of optimum tilt angles of solar collectors determined at yearly, seasonal and monthly levels," Energy Conversion and Management, vol. 97, pp. 121-131, 2015.

[12] W. G. Le Roux, "Optimum tilt and azimuth angles for fixed solar collectors in South Africa using measured data," Renewable Energy, vol. 96, pp. 603-612, 2016.

[13] Y.-M. Chen, C.-H. Lee, and H.-C. Wu, "Calculation of the optimum installation angle for fixed solar-cell panels based on the genetic algorithm and the simulated-annealing method," IEEE Transactions on Energy Conversion, vol. 20, no. 2, pp. 467-473, 2005.

[14] H. Moghadam, F. F. Tabrizi, and A. Z. Sharak, "Optimization of solar flat collector inclination," Desalination, vol. 265, no. 1-3, pp. 107-111, 2011.

[15] Y. Lv, P. Si, X. Rong, J. Yan, Y. Feng, and X. Zhu, "Determination of optimum tilt angle and orientation for solar collectors based on effective solar heat collection," Applied energy, vol. 219, pp. 11-19, 2018.

[16] Z. Yasmeen, G. Rasul, and M. Zahid, "Impact of aerosols on winter fog of Pakistan," Pak. J. Meteor., vol. 8, no. 16, 2012.

[17] M. Aslam, "Fog hazards in Punjab," Pakistan Journal of Meteorology, vol. 8, no. 16, 2012.

[18] M. U. Yousuf and M. Umair, "Development of diffuse solar radiation models using measured

data," International Journal of Green Energy, vol. 11, no. 15, pp. 1-12, 2018.

[19] M. U. Yousuf, M. Umair, and M. Uzair, "Estimating the average diffuse solar radiation based on multiple parameters: a case study of arid climate zone of Pakistan," International Journal of Ambient Energy, vol. 43, no. 1, pp. 1615-1625, 2022.

[20] S. Salma, S. Rehman, and M. Shah, "Rainfall trends in different climate zones of Pakistan," Pakistan Journal of Meteorology, vol. 9, no. 17, 2012.

[21] F. Benford and J. E. Bock, A time analysis of sunshine. General electric Company, Research laboratory, 1938.

[22] J. A. Duffie and W. A. Beckman, Solar engineering of thermal processes. John Wiley and Sons, 2013.

[23] S. Freitas, C. Catita, P. Redweik, and M. C. Brito, "Modelling solar potential in the urban environment: State-of-the-art review," Renewable and Sustainable Energy Reviews, vol. 41, pp. 915-931, 2015.

[24] F. Li et al., "Evaluation of solar radiation models on vertical surface for building photovoltaic applications in Beijing," IET Renewable Power Generation, vol. 16, no. 8, pp. 1792-1807, 2022.

[25] R. Perez, P. Ineichen, R. Seals, J. Michalsky, and R. Stewart, "Modeling daylight availability and irradiance components from direct and global irradiance," Solar energy, vol. 44, no. 5, pp. 271-289, 1990.

[26] R. Perez, R. Seals, and R. Stewart, "Assessing the load matching capability of photovoltaics for US utilities based upon satellite-derived insolation data," in Photovoltaic Specialists Conference, 1993., Conference Record of the Twenty Third IEEE, 1993: IEEE, pp. 1146-1151.

[27] J. Spencer, "Fourier series representation of the position of the sun," Search, vol. 2, no. 5, pp. 172-172, 1971.

[28] M. Iqbal, An introduction to solar radiation. Elsevier, 2012.

[29] D. Erbs, S. Klein, and J. Duffie, "Estimation of the diffuse radiation fraction for hourly, daily and monthly-average global radiation," Solar energy, vol. 28, no. 4, pp. 293-302, 1982.

[30] K. M. Ng, N. M. Adam, O. Inayatullah, and M. Z. A. Ab Kadir, "Assessment of solar radiation on diversely oriented surfaces and optimum tilts for solar absorbers in Malaysian tropical latitude," International Journal of Energy and Environmental Engineering, vol. 5, no. 1, p. 5, 2014.

[31] "NASA Prediction Of Worldwide Energy Resources." https://power.larc.nasa.gov/data-access-viewer/ (accessed).

7. Annexure

Fig. A. Contour Plots of monthly average daily radiation for tilt angle vs azimuth angles for following cities are shown below.

6.1 Karachi

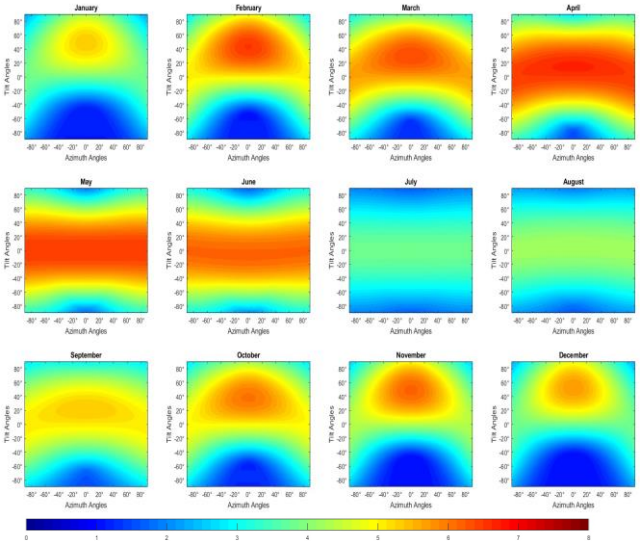

6.2 Multan

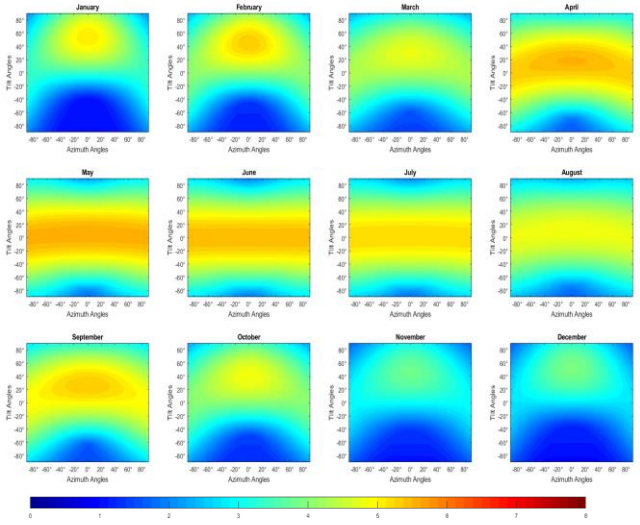

6.3 Quetta

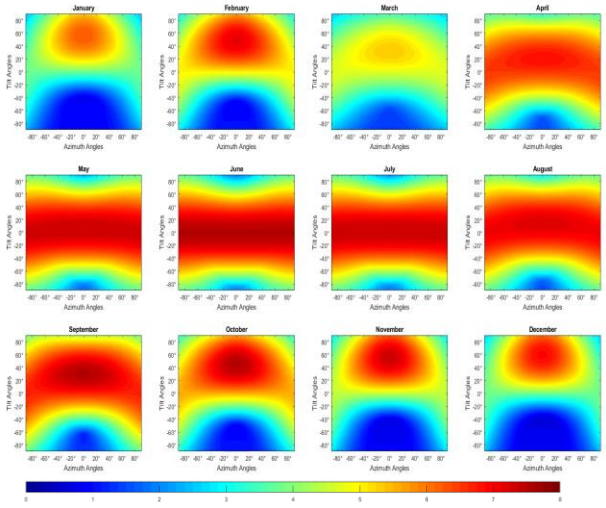

6.4 Peshawar